Received: 7 December 2022 | Revised: 23 May 2023 | Accepted: 12 October 2023

DOI: 10.1002/mma.9750

RESEARCH ARTICLE

WILEY

Galerkin spectral method for linear second-kind Volterra integral equations with weakly singular kernels on large intervals

Walid Remili[1] | **Azedine Rahmoune**[1] | **Chenkuan Li**[2]

[1]Department of Mathematics, Faculty of Mathematics and Informatics, University Mohamed El Bachir El Ibrahimi of Bordj Bou Arreridj, El Anasser, Algeria

[2]Department of Mathematics and Computer Science, Brandon University, Brandon, Manitoba, Canada

Correspondence
Azedine Rahmoune, Department of Mathematics, Faculty of Mathematics and Informatics, University Mohamed El Bachir El Ibrahimi of Bordj Bou Arreridj, El Anasser 34030, Algeria.
Email: a.rahmoune@univ-bba.dz

Communicated by: T. Monovasilis

Funding information
Chenkuan Li is supported by the Natural Sciences and Engineering Research Council of Canada (Grant 2019-03907).

This paper considers the Galerkin spectral method for solving linear second-kind Volterra integral equations with weakly singular kernels on large intervals. By using some variable substitutions, we transform the mentioned equation into an equivalent semi-infinite integral equation with nonsingular kernel, so that the inner products from the Galerkin procedure could be evaluated by means of Gaussian quadrature based on scaled Laguerre polynomials. Furthermore, the error analysis is based on the Gamma function and provided in the weighted L^2-norm, which shows the spectral rate of convergence is attained. Moreover, several numerical experiments are presented to validate the theoretical results.

KEYWORDS

Abel's equations, Galerkin method, scaled Laguerre polynomials, Volterra integral equations, weakly singular kernel

MSC CLASSIFICATION

45D05, 65R20, 33C45, 41A25

1 | INTRODUCTION

The purpose of this paper is to study the second-kind weakly singular Volterra integral equations (WSVIEs) of the forms:

$$u(t) = f(t) + \int_0^t (t-s)^{-\alpha} k(t,s)u(s)ds,\ t \in I, \tag{1}$$

where $I = [0, T]$, $\alpha \in (0, 1)$, $f(t)$ and $k(t, s)$ are given continuous functions, and $u(t)$ is an unknown function that needs to be determined. The WSVIEs (1) have essential applications in various fields of science and engineering, such as seismology, heat conduction, chemical reactions, electrochemistry, crystal growth, physics, and astrophysics [1–9]. Besides, it is well-known that such equations can also arise as solutions to a large class of initial and boundary value problems [10].

Many authors have discussed the existence, uniqueness, and regularity of solutions for a class of WSVIEs, including important special cases, in different functional spaces [10–14]. Recently, Li and Beaudin [15] studied the uniqueness of solutions of the second-kind Abel integral equation with variable coefficients in $L(I)$ and Abel's system in $L(I) \times L(I)$, respectively. Further, Li and Srivastava investigated the uniqueness of solutions to the generalized Abel integral equations in Banach spaces [16].

Owing to the weakly singular nature of its kernel, Equation (1) has an infinite set of singular points when s is near t, an analytical solution cannot be obtained except for special cases [17–19], so numerical methods are highly desired. Despite these difficulties, various methods have been developed and successfully applied, such as Jacobi spectral collocation method [20], piecewise polynomial collocation method [21], collocation method based on the globally continuous piecewise polynomials [22], multi-domain spectral collocation method based on nonpolynomials approximations [23], Block-pulse functions approach [24], hp-version of the discontinuous Galerkin time-stepping method [25], and discontinuous Galerkin approximations [26]. For further methods concerning nonlinear WSVIEs, interested readers are referred, for instance, to [27–30] and the references therein.

Although each of these methods has its own advantages, most of them are not suitable for large intervals, which can limit their usefulness and applications in many areas. For example, in astrophysics and heat transfer, the interval of interest may span a large distance or time period. In these cases, solving the WSVIEs on a smaller interval may lead to inaccurate results, as important features of the solution may be missed and lead to loss of accuracy in the solution. So, the main aim of this paper is to provide an efficient spectral Galerkin approach to solving Equation (1) on large intervals, using scaled Laguerre polynomials (SLPs). In order to achieve our goal and remove the singularity near the diagonal, we first use an appropriate exponential mapping, which transforms the singular integral operator of Equation (1) to an equivalent nonsingular kernel operator, but defined on the half line, and then use the scaled Gauss–Laguerre quadrature rule to approximate the latter. Moreover, we establish the convergence analysis for the approximate and iterated approximate solutions of Equation (1) in scaled Laguerre–Galerkin method with order $\mathcal{O}((\beta N)^{-\frac{m}{2}})$, where m is the smoothness degree of the solution, N is the highest degree of the SLPs used in the approximation, and β is a positive scaling factor which can be used to fine-tune the spacing of collocation points.

The rest of paper is organized as follows. Section 2 introduces the theoretical frameworks of our study. Sections 2.1 and 2.2 mainly describe SLPs approximations and Galerkin method in order to consider the approximate solution of Equation (1). In addition, the convergence results are presented in Section 2.3. Finally, we present numerical experiment results to demonstrate feasibility of the suggested technique in Section 3 and further summarize the entire paper in Section 4.

2 | THEORETICAL FRAMEWORK

Let $L^2_{w_\beta}(\mathbb{R}_+)$ be a weighted Hilbert space, for an arbitrary positive real number $\beta > 0$ and $w_\beta(t) = e^{-\beta t} > 0$, defined as

$$L^2_{w_\beta}(\mathbb{R}_+) = \left\{ u \,|\, u \text{ is measurable on } \mathbb{R}_+ \text{ and } \|u\|_{w_\beta} < \infty \right\}, \tag{2}$$

with the following inner product and norm:

$$(u, v)_{w_\beta} = \int_0^\infty u(t)v(t)w_\beta(t)dt, \ \ \|u\|_{w_\beta} = (u, u)^{\frac{1}{2}}_{w_\beta}. \tag{3}$$

Consider the following integral operator equation:

$$u(t) - \mathcal{K}u(t) = f(t), \ t \in [0, T], \tag{4}$$

where

$$\mathcal{K}u(t) = \int_0^t (t - s)^{-\alpha} k(t, s)u(s)ds.$$

In order to avoid the singularity, we consider a transformation $s(.,.) : [0, T] \times \mathbb{R}_+ \to [0, t]$ by

$$s = \theta_t(x) = t(1 - e^{-x}).$$

Then, the integral part in Equation (1) becomes

$$\int_0^t (t-s)^{-\alpha} k(t,s)u(s)ds = \int_0^\infty k(t,\theta_t(x))t^{1-\alpha}e^{-(1-\alpha)x}u(\theta_t(x))dx. \tag{5}$$

Proposition 1. *Assume that*

$$\max_{0\le t\le T} \int_0^t (t-s)^{-\alpha}|k(t,s)|^2 ds = M < \infty. \tag{6}$$

Then, we have

$$\|\mathcal{K}u\|_{w_\beta} \le M\beta^{\alpha-1}\Gamma(1-\alpha)\|u\|_{w_\beta}, \tag{7}$$

where $\Gamma(.)$ *is the Gamma function defined by*

$$\Gamma(\nu) = \int_0^\infty t^{\nu-1}e^{-t}dt.$$

Proof. By applying the Cauchy–Schwarz inequality, we get

$$\begin{aligned}|\mathcal{K}u(t)|^2 e^{-\beta t} &\le \left(\int_0^t (t-s)^{-\alpha}|k(t,s)|^2 ds\right)\left(\int_0^t (t-s)^{-\alpha}e^{-\beta(t-s)}|u(s)|^2 e^{-\beta s}ds\right)\\ &\le M\left(\int_{-\infty}^\infty (t-s)^{-\alpha}e^{-\beta(t-s)}|u(s)|^2\chi_{[0,t]}(s)e^{-\beta s}ds\right).\end{aligned}$$

Let us define

$$g(t) = t^{-\alpha}e^{-\beta t}H(t), \tag{8}$$

where H is the Heaviside function, and let

$$\tilde{u}(s) = |u(s)|^2\chi_{[0,t]}(s)e^{-\beta s}, \tag{9}$$

so that we can write

$$(g\star\tilde{u})(t) := \int_{-\infty}^\infty g(t-s)\tilde{u}(s)ds.$$

Obviously, we have $\|\tilde{u}\|_1 = \|\tilde{u}\|_{1,(-\infty,\infty)}$. Moreover, it's not hard to prove that

$$\|g\|_1 = \beta^{\alpha-1}\Gamma(1-\alpha).$$

Indeed,

$$\int_0^\infty t^{-\alpha}e^{-\beta t}dt = \beta^{\alpha-1}\int_0^\infty t^{-\alpha}e^{-t}dt = \beta^{\alpha-1}\Gamma(1-\alpha).$$

Hence, by using Young's theorem 4.15 [31, p. 104], we obtain

$$\|g\star\tilde{u}\|_1 \le \|g\|_1\|\tilde{u}\|_1 = \beta^{\alpha-1}\Gamma(1-\alpha)\|\tilde{u}\|_1. \tag{10}$$

This implies

$$\|\mathcal{K}u\|_{w_\beta} \le M\|g\star\tilde{u}\|_1 \le M\beta^{\alpha-1}\Gamma(1-\alpha)\|u\|_{w_\beta}. \tag{11}$$

This completes the proof of Proposition 1. □

Next, consider the SLPs of degree n defined by (see, e.g., [32])

$$\mathcal{L}_n^\beta(t) = \frac{1}{n!} e^{\beta t} \partial_t^n (t^n e^{-\beta t}),\ n \in \mathbb{N}, t \in \mathbb{R}_+, \tag{12}$$

with the following properties:

$$\mathcal{L}_0^\beta(t) = 1,\ \mathcal{L}_1^\beta(t) = (1-\beta t); (n+1)\mathcal{L}_{n+1}^\beta(t) = (2n+1-\beta t)\mathcal{L}_n^\beta(t) - n\mathcal{L}_{n-1}^\beta(t),\ n \geq 1, \tag{13}$$

the leading coefficient of $\mathcal{L}_n^\beta(t)$ is $(-\beta^n)/n!$ and $\mathcal{L}_n^\beta(0) = 1$. In the special case $\beta = 1$, we obtain the classical Laguerre polynomials $L_n(t)$. Moreover, we have

$$\mathcal{L}_n^\beta(t) = L_n(\beta t),\ n \in \mathbb{N}.$$

Applying the weight function $w_\beta(t) = e^{-\beta t}$, we have the orthogonality relationship:

$$\int_0^\infty \mathcal{L}_n^\beta(t)\mathcal{L}_m^\beta(t) e^{-\beta t} dx = \frac{1}{\beta}\delta_{n,m}, \tag{14}$$

where $\delta_{n,m}$ is the Kronecker function. In addition, the set of SLPs forms a complete $L^2_{w_\beta}(\mathbb{R}_+)$-orthogonal basis. For any function $u \in L^2_{w_\beta}(\mathbb{R}_+)$, it can be expanded in series of SLPs:

$$u(t) = \sum_{n=0}^\infty u_n^\beta \mathcal{L}_n^\beta(t),\ u_n^\beta = \beta \int_0^\infty u(t)\mathcal{L}_n^\beta(t) w_\beta(t) dt. \tag{15}$$

2.1 | SLP approximations

Now, we define the weighted orthogonal projection operator $P_N^\beta : L^2_{w_\beta}(\mathbb{R}_+) \to \mathbb{P}_N$ as

$$(P_N^\beta u - u, \phi)_{w_\beta} = 0,\ \forall \phi \in \mathbb{P}_N, \tag{16}$$

where

$$P_N^\beta u(t) = \sum_{n=0}^N u_{n,N}^\beta \mathcal{L}_n^\beta(t), \tag{17}$$

and $\mathbb{P}_N$ denotes the set of all SLPs on $\mathbb{R}_+$ with a degree $\leq N$.

Let $\xi_{G,j}^{\beta,N}$ and $\xi_{R,j}^{\beta,N}$, $0 \leq j \leq N$ be the zeros of $\mathcal{L}_{N+1}^\beta(t)$ and $t\partial_t\mathcal{L}_{N+1}^\beta(t)$, respectively. They are arranged in ascending order. Denote $\omega_{Z,j}^{\beta,N}$, $0 \leq j \leq N$, $Z = G, R$, the corresponding Christoffel numbers, such that

$$\int_0^\infty \phi(t) w_\beta(t) dt = \sum_{j=0}^N \phi\left(\xi_{Z,j}^{\beta,N}\right) \omega_{Z,j}^{\beta,N}\ \forall \phi \in \mathbb{P}_{2N+\lambda_Z}, \tag{18}$$

where $\lambda_Z = 1$ and 0 for $Z = G$ and $Z = R$, respectively. In fact, according to [32], the scaled Laguerre–Gauss and Laguerre–Gauss–Radau weights are given, respectively, by

$$\omega_{G,j}^{\beta,N} = \frac{1}{\xi_{G,j}^{\beta,N}\left[\partial_t \mathcal{L}_{N+1}^\beta\left(\xi_{G,j}^{\beta,N}\right)\right]^2}, 0 \leq j \leq N, \tag{19}$$

and

$$\omega_{R,j}^{\beta,N} = \begin{cases} \frac{1}{\beta(N+1)}, & j = 0, \\ \frac{1}{(N+1)\mathcal{L}_{N+1}^{\beta}\left(\xi_{R,j}^{\beta,N}\right)\partial_t \mathcal{L}_N^{\beta}\left(\xi_{R,j}^{\beta,N}\right)}, & 1 \le j \le N. \end{cases} \tag{20}$$

We further introduce the discrete inner product and discrete norm:

$$(u,v)_{w_\beta,Z,N} = \sum_{j=0}^{N} u\left(\xi_{Z,j}^{\beta,N}\right) v\left(\xi_{Z,j}^{\beta}\right) \omega_{Z,j}^{\beta,N}, \ \|u\|_{w_\beta,Z,N} = (u,u)_{w_\beta,Z,N}^{1/2}. \tag{21}$$

From (18) and (21), we infer that

$$(u,v)_{w_\beta} = (u,v)_{w_\beta,Z,N} \text{ and } \|u\|_{w_\beta} = \|u\|_{w_\beta,Z,N}, \forall uv \in \mathbb{P}_{2N+\lambda_Z}. \tag{22}$$

In order to describe the approximation results, we introduce the weighted space $H_\beta^m(\mathbb{R}_+)$. For any integer $m \ge 0$, we define the weighted Sobolev space

$$H_\beta^m(\mathbb{R}_+) = \left\{ u \,|\, t^{\frac{k}{2}} \partial_t^k u \in L_{w_\beta}^2(\mathbb{R}_+), 0 \le k \le m \right\}, \tag{23}$$

equipped with the following semi-norm and norm:

$$|u|_{H_\beta^m(\mathbb{R}_+)} = \left\| t^{\frac{m}{2}} \partial_t^m u \right\|_{w_\beta}, \ \|u\|_{H_\beta^m(\mathbb{R}_+)} = \left(\sum_{k=0}^{m} |u|_{H_\beta^k(\mathbb{R}_+)}^2 \right)^{1/2}.$$

The following lemma gives an error estimation between the approximate and exact solutions (see Theorem 2.1 in [33])

Lemma 1. *For any $u \in H_\beta^m(\mathbb{R}_+)$ and integer $m \ge 1$,*

$$\left\| P_N^\beta u - u \right\|_{w_\beta} \le c(\beta N)^{-\frac{m}{2}} |u|_{H_\beta^m(\mathbb{R}_+)}, \tag{24}$$

where c is a positive constant independent of N and u.

2.2 | Scaled Laguerre–Galerkin method

In this subsection, the Galerkin method by means of the SLPs is applied for solving Equation (1), where the solution u is assumed to belong to $L_{w_\beta}^2(\mathbb{R}_+)$. Then, the projection u can be expanded by a finite series of SLPs as follows:

$$P_N^\beta u(t) = \sum_{n=0}^{N} u_{n,N}^\beta \mathcal{L}_n^\beta(t). \tag{25}$$

Substituting (25) and (5) into the integral equation (1), we obtain the residual function:

$$R_N^\beta(t) = \sum_{n=0}^{N} u_{n,N}^\beta \left(\mathcal{L}_n^\beta(t) - \int_0^\infty k(t,\theta_t(x)) t^{1-\alpha} e^{-(1-\alpha)x} \mathcal{L}_n^\beta(\theta_t(x)) dx \right) - f(t), \tag{26}$$

satisfying $\left(R_N^\beta, \mathcal{L}_m^\beta\right)_{w_\beta} = 0$, for $0 \le m \le N$. Let

$$h_n^\beta(t) = \int_0^\infty k(t,\theta_t(x)) t^{1-\alpha} e^{-(1-\alpha)x} \mathcal{L}_n^\beta(\theta_t(x)) dx = \left(t^{1-\alpha} k(t,\theta_t(.)), \mathcal{L}_n^\beta(\theta_t(.)) \right)_{w_{(1-\alpha)}}, \tag{27}$$

then Equation (26) can be written as

$$R_N^{\beta}(t) = \sum_{n=0}^{N} u_{n,N}^{\beta} \left(\mathcal{L}_n^{\beta}(t) - h_n^{\beta}(t) \right) - f(t). \tag{28}$$

Multiplying (28) by $\mathcal{L}_m^{\beta}(t) w_{\beta}(t)$ to both sides and then integrating from zero to infinity, we get

$$\sum_{n=0}^{N} u_{n,N}^{\beta} \left\{ \left(\mathcal{L}_n^{\beta}, \mathcal{L}_m^{\beta} \right)_{w_{\beta}} - \left(h_n^{\beta}, \mathcal{L}_m^{\beta} \right)_{w_{\beta}} \right\} = \left(f, \mathcal{L}_m^{\beta} \right)_{w_{\beta}}, \tag{29}$$

by noting the fact that

$$\left(R_N^{\beta}, \mathcal{L}_m^{\beta} \right)_{w_{\beta}} = 0, \ m = 0, 1, \ \dots \ , .$$

Using the orthogonality condition of the SLPs, Equation (29) turns out to be

$$\frac{u_{m,N}^{\beta}}{\beta} - \sum_{n=0}^{N} u_{n,N}^{\beta} \left(h_n^{\beta}, \mathcal{L}_m^{\beta} \right)_{w_{\beta}} = \left(f, \mathcal{L}_m^{\beta} \right)_{w_{\beta}}, \ 0 \le m \le N. \tag{30}$$

To solve (30) in practice, we must numerically evaluate these occurred inner products. Thus, use the numerical integration scheme (21) and (22) based on the set of scaled Laguerre–Gauss nodes and weights $\left\{ \xi_{Z,j}^{\beta,N}, \omega_{Z,j}^{\beta,N} \right\}_{j=0}^{N}$ as follows:

$$\left(h_n^{\beta}, \mathcal{L}_m^{\beta} \right)_{w_{\beta}} \approx \sum_{j=0}^{N} h_n^{\beta} \left(\xi_{Z,j}^{\beta,N} \right) \mathcal{L}_m^{\beta} \left(\xi_{Z,j}^{\beta,N} \right) \omega_{Z,j}^{\beta,N}, \tag{31}$$

$$\left(f, \mathcal{L}_m^{\beta} \right)_{w_{\beta}} \approx \sum_{j=0}^{N} f \left(\xi_{Z,j}^{\beta,N} \right) \mathcal{L}_m^{\beta} \left(\xi_{Z,j}^{\beta,N} \right) \omega_{Z,j}^{\beta,N}, \tag{32}$$

where, according to (27), we have

$$h_n^{\beta} \left(\xi_{Z,j}^{\beta,N} \right) \approx \left(\xi_{Z,j}^{\beta,N} \right)^{1-\alpha} \sum_{k=0}^{N} k \left(\xi_{Z,j}^{\beta,N}, \theta_{\xi_{Z,j}^{\beta,N}} \left(\xi_{Z,k}^{1-\alpha,N} \right) \right) \mathcal{L}_n^{\beta} \left(\theta_{\xi_{Z,j}^{\beta,N}} \left(\xi_{Z,k}^{1-\alpha,N} \right) \right) \omega_{Z,k}^{1-\alpha,N}.$$

Let us denote

$$\mathbf{u} = \left[u_{0,N}^{\beta}, \ \dots \ , u_{N,N}^{\beta} \right]^{\mathrm{T}}, \mathbf{f} = \left[f \left(\xi_{Z,j}^{\beta,N} \right), \ \dots \ , f \left(\xi_{Z,j}^{\beta,N} \right) \right]^{\mathrm{T}}, \mathbf{w} = \mathrm{diag} \left(\left(\omega_{Z,k}^{1-\alpha,N} \right)_{k=0}^{N} \right),$$

$$\mathbf{D} = \left\{ \left(\mathcal{L}_0^{\beta} \left(\xi_{Z,j}^{\beta,N} \right), \ \dots \ , \mathcal{L}_N^{\beta} \left(\xi_{Z,j}^{\beta,N} \right) \right) \right\}_{j,n=0}^{N}, \mathbf{M} = \left(\left(\xi_{Z,j}^{\beta,N} \right)^{1-\alpha} k \left(\xi_{Z,j}^{\beta,N}, \theta_{\xi_{Z,j}^{\beta,N}} \left(\xi_{Z,k}^{1-\alpha,N} \right) \right) \right)_{j,k=0}^{N},$$

and

$$\mathbf{W} = \mathrm{diag} \left(\left(\omega_{Z,j}^{\beta,N} \right)_{j=0}^{N} \right), \mathbf{d} = \left\{ \left(\mathcal{L}_0^{\beta} \left(\theta_{\xi_{Z,j}^{\beta,N}} \left(\xi_{Z,k}^{1-\alpha,N} \right) \right), \ \dots \ , \mathcal{L}_N^{\beta} (\theta_{\xi_{Z,j}^{\beta,N}} \left(\xi_{Z,k}^{1-\alpha,N} \right) \right) \right\}_{j,k=0}^{N}.$$

Then, (30) leads to the matrix system

$$(\mathbf{I}/\beta - \mathbf{DWMwd}')\mathbf{u} = \mathbf{DWf}. \tag{33}$$

2.3 | Convergence analysis

We are ready to present the convergence analysis of the following Galerkin solution:

$$u_N^{\beta} = P_N^{\beta} \mathcal{K} u_N^{\beta} + P_N^{\beta} f. \tag{34}$$

To begin, we define the iterated solution as

$$\tilde{u}_N^\beta = \mathcal{K} u_N^\beta + f. \tag{35}$$

Applying P_N^β to both sides of Equation (35), we obtain

$$P_N^\beta \tilde{u}_N = P_N^\beta \mathcal{K} u_N + P_N^\beta f. \tag{36}$$

It follows that $P_N^\beta \tilde{u}_N^\beta = u_N^\beta$ from Equations (34) and (36). So, the iterated solution $\tilde{u}_N^\beta$ satisfies the following equation:

$$\tilde{u}_N^\beta = \mathcal{K} P_N^\beta \tilde{u}_N^\beta + f. \tag{37}$$

We quote the following lemma from [34, Theorem 2.3.5].

Lemma 2. *Let $\mathcal{X}$ be a Banach space. Assume $L : \mathcal{X} \to \mathcal{X}$ is bounded and $(I - L) : \mathcal{X} \to \mathcal{X}$ is one to one and onto. Further assume $\|L - L_n\| \to 0$ as $n \to \infty$. Then, for all sufficiently large n, the operator $(I - L_n)^{-1}$ exists and is uniformly bounded on $\mathcal{X}$.*

Next, we prove the following lemma, which is useful in our convergence analysis.

Lemma 3. *Consider $0 < \alpha < 1$ fixed, and assume that $I - \mathcal{K} : L^2_{w_\beta}(\mathbb{R}_+) \to L^2_{w_\beta}(\mathbb{R}_+)$ is one to one and onto; then, we have*

$$\|\mathcal{K} - \mathcal{K} P_N^\beta\|_{w_\beta} \to 0, \quad as\ N \to \infty. \tag{38}$$

Furthermore, for all sufficiently large N, the operator $\left(I - \mathcal{K} P_N^\beta\right)^{-1}$ exists as a bounded operator from $L^2_{w_\beta}(\mathbb{R}_+)$ to $L^2_{w_\beta}(\mathbb{R}_+)$ and

$$\left\| \left(I - \mathcal{K} P_N^\beta\right)^{-1} \right\|_{w_\beta} < +\infty. \tag{39}$$

Proof. According to Proposition 1, for all $u \in L^2_{w_\beta}(\mathbb{R}_+)$, we have

$$\left\| \mathcal{K} u - \mathcal{K} P_N^\beta u \right\|_{w_\beta} = \left\| \mathcal{K} \left(u - P_N^\beta u \right) \right\|_{w_\beta} \le M \beta^{\alpha-1} \Gamma(1-\alpha) \left\| P_N^\beta u - u \right\|_{w_\beta}. \tag{40}$$

From Lemma 1, we come to

$$\left\| \mathcal{K} u - \mathcal{K} P_N^\beta u \right\|_{w_\beta} \le c M \beta^{\alpha-1} \Gamma(1-\alpha) (\beta N)^{-\frac{m}{2}} |u|_{H^m_\beta(\mathbb{R}_+)}. \tag{41}$$

Since $\Gamma(1-\alpha) < \infty$ for every fixed $\alpha \in (0,1)$, then $\left\| \mathcal{K} - \mathcal{K} P_N^\beta \right\|_{w_\beta} \to 0$, as $N \to \infty$. By Lemma 2, the inequality (39) holds. This completes the proof of Lemma 3. □

In the following, we would like to present the estimation analysis of u_N^β and $\tilde{u}_N^\beta$ to the exact solution u by the above lemmas.

Theorem 1. *Let u be the exact solution of the integral equation $(I - \mathcal{K})u = f$, the approximate solution u_N^β be obtained by using the spectral Galerkin method for solving $\left(I - P_N^\beta \mathcal{K}\right) u_N^\beta = P_N^\beta f$, and the iterated solution $\tilde{u}_N^\beta$ satisfy $\left(I - \mathcal{K} P_N^\beta\right) \tilde{u}_N^\beta = f$. Then,*

$$\left\| u - \tilde{u}_N^\beta \right\|_{w_\beta} \le \tilde{C}_{\alpha,\beta} (\beta N)^{-\frac{m}{2}} |u|_{H^m_\beta(\mathbb{R}_+)}, \tag{42}$$

and

$$\left\| u - u_N^\beta \right\|_{w_\beta} \le C_{\alpha,\beta} (\beta N)^{-\frac{m}{2}} |u|_{H^m_\beta(\mathbb{R}_+)}, \tag{43}$$

where $\tilde{C}_{\alpha,\beta}$ and $C_{\alpha,\beta}$ are positive constants depending on α and β.

Proof. From the integral equation

$$u = \mathcal{K}u + f, \tag{44}$$

we get

$$u - \tilde{u}_N^\beta = \mathcal{K}u - \mathcal{K}P_N^\beta \tilde{u}_N^\beta = \mathcal{K}u - \mathcal{K}P_N^\beta u + \mathcal{K}P_N^\beta u - \mathcal{K}P_N^\beta \tilde{u}_N^\beta, \tag{45}$$

and

$$u - \tilde{u}_N^\beta = \left(I - \mathcal{K}P_N^\beta\right)^{-1} \mathcal{K}(I - P_N^\beta)u. \tag{46}$$

Hence,

$$\left\|u - \tilde{u}_N^\beta\right\|_{w_\beta} \leq \left\|\left(I - \mathcal{K}P_N^\beta\right)^{-1}\right\|_{w_\beta} \left\|\mathcal{K}\left(I - P_N^\beta\right)u\right\|_{w_\beta}. \tag{47}$$

It follows from Proposition 1 and Lemma 1 that

$$\left\|u - \tilde{u}_N^\beta\right\|_{w_\beta} \leq \left\|\left(I - \mathcal{K}P_N^\beta\right)^{-1}\right\|_{w_\beta} M\beta^{\alpha-1}\Gamma(1-\alpha)\left\|u - P_N^\beta u\right\|_{w_\beta}, \tag{48}$$

$$\leq \left\|\left(I - \mathcal{K}P_N^\beta\right)^{-1}\right\|_{w_\beta} M\beta^{\alpha-1}\Gamma(1-\alpha)c(\beta N)^{-\frac{m}{2}}|u|_{H_\beta^m(\mathbb{R}_+)}. \tag{49}$$

Now, we estimate an error between the approximate and exact solutions where $u_N^\beta = P_N^\beta \tilde{u}_N^\beta$

$$\begin{aligned} u - u_N^\beta &= u - P_N^\beta \tilde{u}_N^\beta \\ &= u - P_N^\beta u + P_N^\beta u - P_N^\beta \tilde{u}_N^\beta. \end{aligned} \tag{50}$$

This implies

$$\|u - u_N^\beta\|_{w_\beta} \leq \|u - P_N^\beta u\|_{w_\beta} + \|P_N^\beta\|_{w_\beta}\left\|u - \tilde{u}_N^\beta\right\|_{w_\beta}. \tag{51}$$

From (48), (51), and Lemma 1, we get

$$\begin{aligned} \|u - u_N^\beta\|_{w_\beta} &\leq \left(1 + \|P_N^\beta\|_{w_\beta}\|(I - \mathcal{K}P_N^\beta)^{-1}\|_{w_\beta} M\beta^{\alpha-1}\Gamma(1-\alpha)\right)\|u - P_N^\beta u\|_{w_\beta} \\ &\leq \left(1 + \|(I - \mathcal{K}P_N^\beta)^{-1}\|_{w_\beta} M\beta^{\alpha-1}\Gamma(1-\alpha)\right)c(\beta N)^{-\frac{m}{2}}|u|_{H_\beta^m(\mathbb{R}_+)}. \end{aligned} \tag{52}$$

This completes the proof of Theorem 1. □

TABLE 1 The $L_{w_\beta}^2$-errors for Example 1 with $\alpha = 0.5$ and $n = 1$.

N	4	8	16	32
$\|u - u_N^\beta\|_{w_\beta}$	3.47e−02	1.71e−04	4.22e−09	1.75e−13
$\|u - \tilde{u}_N^\beta\|_{w_\beta}$	3.47e−02	1.71e−04	4.22e−09	1.75e−13

TABLE 2 The maximum absolute errors and CPU time for Example 1 with $\alpha = 0.5$ and $n = 1$.

	$T = 1$		$T = 10$		$T = 20$		
N	$\|u - u_N^\beta\|_\infty$	$\|u - \tilde{u}_N^\beta\|_\infty$	$\|u - u_N^\beta\|_\infty$	$\|u - \tilde{u}_N^\beta\|_\infty$	$\|u - u_N^\beta\|_\infty$	$\|u - \tilde{u}_N^\beta\|_\infty$	CPU (s)
4	1.43e−02	1.22e−02	7.59e−02	5.92e−02	1.44e−01	3.10e−01	0.255482
8	8.03e−05	8.76e−05	3.19e−04	4.13e−04	1.73e−03	3.60e−03	0.268771
16	1.65e−09	1.81e−09	8.37e−09	1.33e−08	3.89e−08	7.57e−08	0.309112
32	4.88e−14	3.82e−14	1.85e−13	4.05e−13	3.88e−12	5.76e−12	0.439622

TABLE 3 The $L_{w_\beta}^2$-errors for Example 1 with $\alpha = 0.5$ and $n = 2$.

N	8	16	32	64
$\|u - u_N^\beta\|_{w_\beta}$	1.05e−01	2.16e−04	7.43e−10	3.39e−12
$\|u - \tilde{u}_N^\beta\|_{w_\beta}$	1.05e−01	2.16e−04	7.43e−10	4.31e−12

	$T = 1$		$T = 10$		$T = 20$		
N	$\|u - u_N^\beta\|_\infty$	$\|u - \tilde{u}_N^\beta\|_\infty$	$\|u - u_N^\beta\|_\infty$	$\|u - \tilde{u}_N^\beta\|_\infty$	$\|u - u_N^\beta\|_\infty$	$\|u - \tilde{u}_N^\beta\|_\infty$	CPU (s)
8	9.86e−03	1.03e−02	3.57e−01	3.59e−01	1.39e+00	1.49e+00	0.319806
16	1.41e−05	1.83e−05	7.44e−04	7.83e−05	2.48e−03	2.76e−03	0.378017
32	8.33e−11	6.41e−11	2.11e−09	2.57e−09	1.54e−08	1.87e−08	0.486933
64	7.06e−13	5.57e−13	6.39e−12	8.41e−12	3.11e−11	6.86e−11	0.978953

TABLE 4 The maximum absolute errors and CPU time for Example 1 with $\alpha = 0.5$ and $n = 2$.

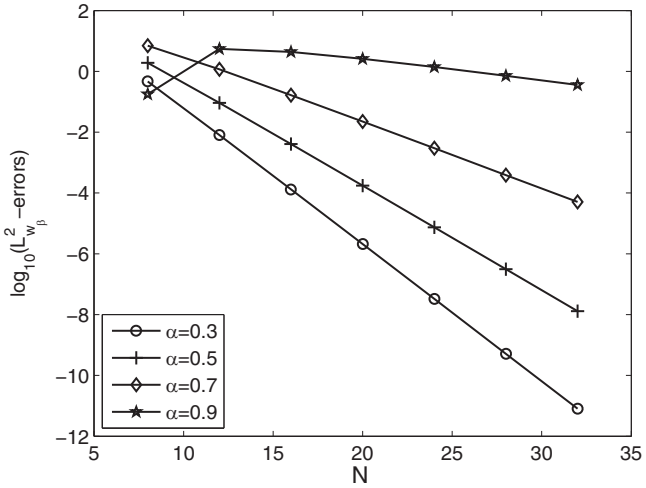

FIGURE 1 Convergence rates of the SLGR method with $\beta = 0.2$: Example 1 for $n = 2$ and various α.

3 | NUMERICAL EXPERIMENTS

We are going to present several examples for solving WSVIEs. The approximate and iterated approximate solutions obtained by the proposed Galerkin method will be compared with the exact solution. The computations are executed with Matlab software on a Core i5-2520M CPU running at 2.5 GHZ and 4 GB RAM. In addition, the CPU times are recorded in seconds.

Example 1. Consider the following linear WSVIEs:

$$u(t) = t^n + t^{n+1-\alpha}B(n+1, 1-\alpha) - \int_0^t (t-s)^{-\alpha}u(s)ds,\ t \in [0, T], \tag{53}$$

where $B(\nu, \lambda)$ is the Beta function defined by

$$B(\nu, \lambda) = \int_0^1 x^{\nu-1}(1-x)^{\lambda-1}dx \text{ for } \nu, \lambda > 0.$$

The exact solution of this problem is $u(t) = t^n$, which is an increasing function on $\mathbb{R}_+$. In Tables 1–4, we display the numerical errors versus N for $n \in \{1, 2\}$, $\alpha = 0.5$, and different values of T, obtained by using the SLGR scheme described above with $\beta = 0.5$. From these numerical results, it can be clearly seen that the error history is decayed according to N and agrees well with the theoretical results, indicating as predicted in Theorem 1 that the numerical solutions will converge faster than any algebraic power. The CPU time remains very low amount in spite of the increment of N. In addition, Figure 1 illustrates that the performance of the method degrades as α is close to 1, since the upper bounds include the Gamma function $\Gamma(1-\alpha)$ and $\Gamma(1-\alpha) \to \infty$ as α is near 1. Figure 2 shows the absolute stability of the proposed method over a large enough interval.

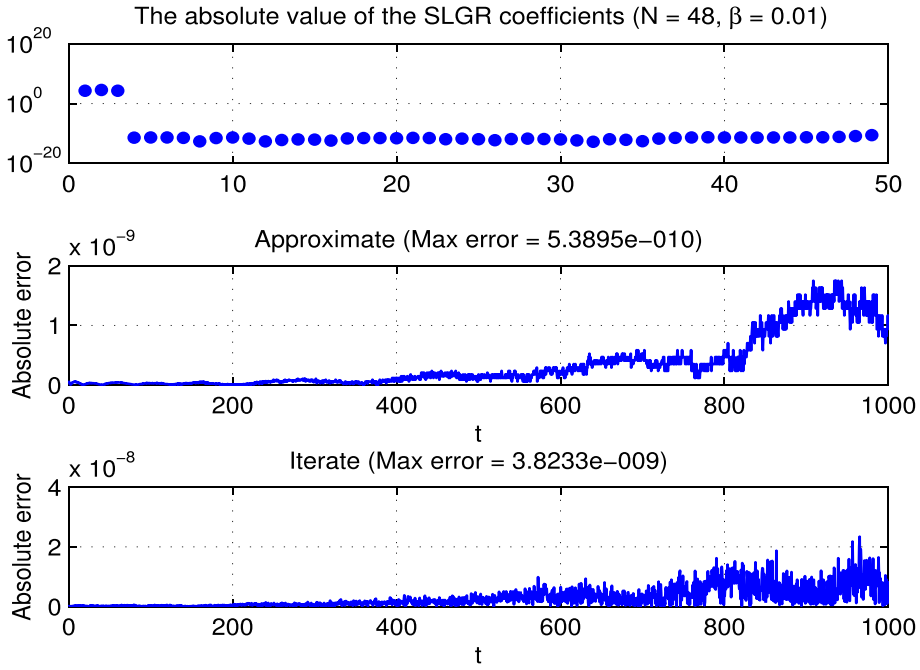

FIGURE 2 Absolute stability of the SLGR method: Example 1 for $n = 2$, $\alpha = 0.5$, and $T = 1000$. [Colour figure can be viewed at wileyonlinelibrary.com]

TABLE 5 Comparison of the absolute errors for Example 2.

	$\lvert u(x) - u_N^{\beta}(x)\rvert$		$\lvert u(x) - \tilde{u}_N^{\beta}(x)\rvert$		**Method in [24]**	
x	$N = 32$	$N = 64$	$N = 32$	$N = 64$	$N = 32$	$N = 64$
0	1.48e−11	1.57e−12	00	00	8.77e−04	7.00e−06
0.2	9.49e−11	4.75e−14	9.96e−11	3.00e−14	5.65e−04	2.07e−06
0.4	3.22e−09	1.96e−12	3.22e−09	1.88e−12	1.70e−06	2.50e−07
0.6	2.44e−08	3.31e−11	2.45e−08	3.30e−11	4.24e−05	7.42e−06
0.8	9.95e−08	2.42e−10	9.95e−08	2.42e−10	5.00e−06	3.99e−05
1	2.86e−07	1.11e−09	2.85e−07	1.11e−09	1.32e−05	3.78e−06

Example 2. Consider

$$u(t) = (t+1)^{-\frac{1}{2}} + \frac{\pi}{8} - \frac{1}{4}\arcsin\left(\frac{1-t}{1+t}\right) - \frac{1}{4}\int_0^t (t-s)^{-\frac{1}{2}} u(s)ds,\ t \in [0, T], \tag{54}$$

whose exact solution is $u(t) = (t+1)^{-\frac{1}{2}}$, which is a very slow decaying function at large distance. For the sake of comparison, Table 5 shows that the absolute errors obtained at some equally-spaced points of the unit interval by using the SLG scheme with $\beta = 6$ are much more better than those previously obtained by using block-pulse function approach [24].

To illustrate the important role of β-parameter, we compare in Figure 3 the exact solution with the numerical ones obtained using the SLG scheme with different values of β. It can be seen that for $N = 8$, both approximate and iterated approximate solutions obtained with $\beta = 1.6$ exhibit an observable error in a neighborhood of the right extremity of the interval, while the numerical solutions obtained with $\beta = 0.6$ are almost identical to the exact solution.

Example 3. Consider

$$u(t) = f(t) + \int_0^t (t-s)^{-\frac{1}{4}}(t+s)e^{-t}u(s)ds,\ t \in [0, T], \tag{55}$$

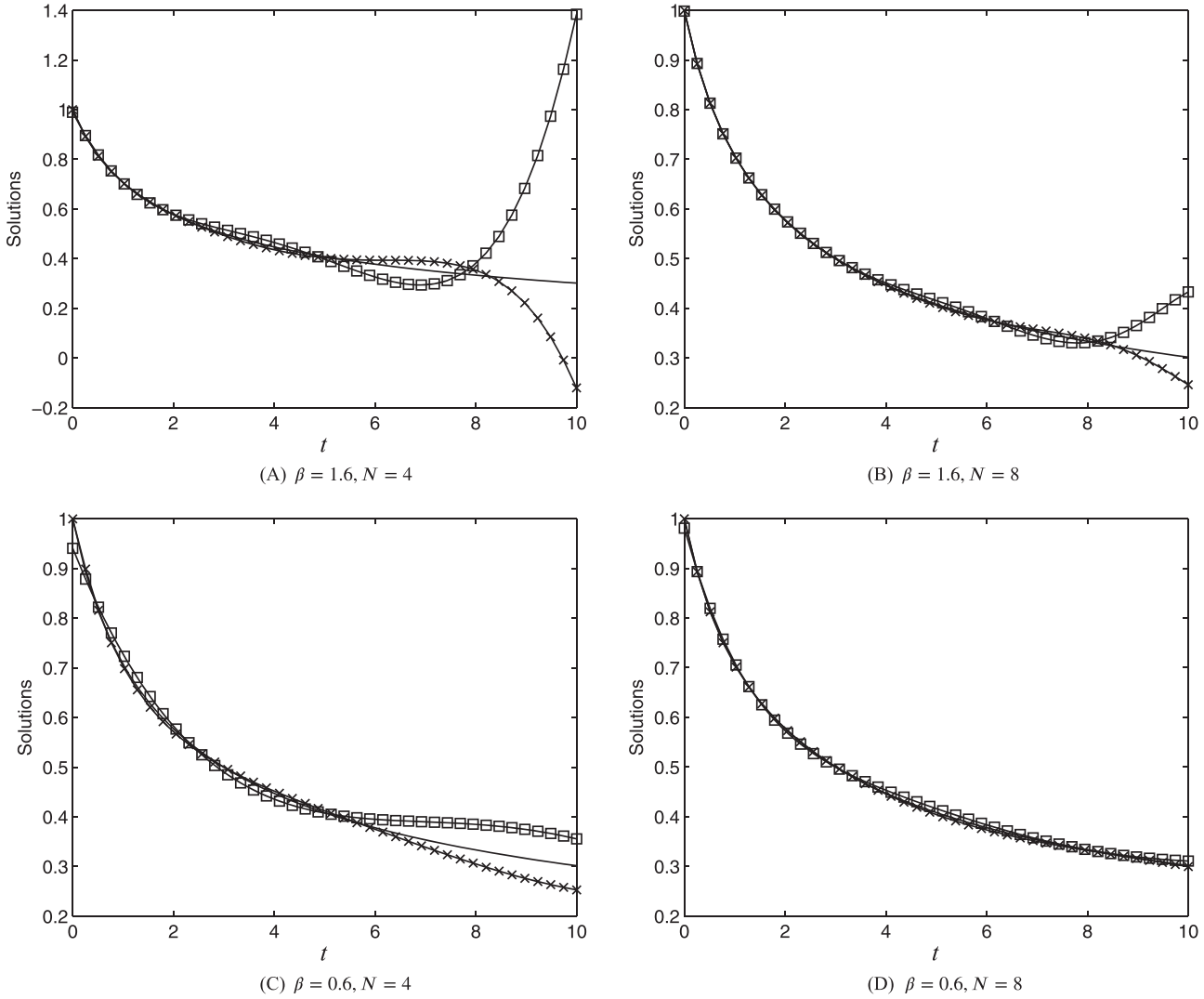

FIGURE 3 Plots of the approximate (square), iterated (cross), and the exact (solid line) solutions of Example 2.

where $f(t)$ is chosen so that the exact solution is $u(t) = (t^2 - c_1 t)(t - c_2)$, with c_1 and c_2 being real constants. Tables 6 and 7 show the numerical errors versus N for $c_1 = T/3$, $c_2 = T/2$ with different values of T, obtained by the SLGR scheme with $\beta = 0.5$.

In Figure 4 (left), we plot $\log_{10}$ of the maximum error of the approximate solution, while on the right, we plot the corresponding $\log_{10}$ of the weighted error for $c_1 = 0.5$, $c_2 = 0.9$, and $T = 1$. The two errors exhibit a similar decay with respect to N. In particular, for larger N ($N \geq 32$), better numerical results can be obtained by choosing suitable $\beta > 1$.

Furthermore, we plot in Figure 5 the absolute errors of the numerical solutions for $c_1 = 250$, $c_2 = 400$, and $T = 500$, obtained with $N = 64$ and different values of β. As we can see from this figure, the approximate solution (left panels) is very sensitive to β-parameter, while conversely for the iterated solution (right panels), the corresponding scheme is more robust and retains a high order of convergence on the whole interval. In order to upgrade the convergence of the approximate solution and avoid this sensitivity, which is actually due to the distribution of the scaled Laguerre–Gauss–Radau nodes that are clustered near the endpoint $t = 0$, it is necessary to adjust the grid points over the large interval (see Figure 6). This means that for fixed N, even if it is small, the scaling strategy can gain better accuracy simply by decreasing β. For example, with $N = 4$ and $\beta = 0.01$, the matrix corresponding to the Galerkin system (33) is diagonal, its condition number is close to one, and the SLGR coefficient matrix is gained as

$$\mathbf{u} = [-1{,}925{,}000 - 1{,}975{,}000\,10{,}000{,}000 - 6{,}000{,}000\,1/93{,}206{,}756]^{\mathrm{T}}.$$

Figure 7 shows that the SLGR method gives us results with higher degree of accuracy.

TABLE 6 The $L^2_{w_\beta}$-errors for Example 3 with $\beta = 0.5$.

	$c_1 = 1/3, c_2 = 1/2$		$c_1 = 10/3, c_2 = 5$		$c_1 = 20/3, c_2 = 10$	
N	$\|u - u_N^\beta\|_{w_\beta}$	$\|u - \tilde{u}_N^\beta\|_{w_\beta}$	$\|u - u_N^\beta\|_{w_\beta}$	$\|u - \tilde{u}_N^\beta\|_{w_\beta}$	$\|u - u_N^\beta\|_{w_\beta}$	$\|u - \tilde{u}_N^\beta\|_{w_\beta}$
8	1.41e−02	1.41e−02	8.21e−03	8.21e−03	3.01e−02	3.01e−02
16	3.97e−04	3.97e−04	4.59e−04	4.59e−04	5.29e−04	5.29e−04
32	3.03e−08	3.03e−08	3.05e−08	3.05e−08	3.08e−08	3.08e−08
64	1.85e−12	6.26e−14	1.20e−12	7.16e−14	2.04e−12	2.84e−13

TABLE 7 The maximum absolute errors and CPU time for Example 3 with $\beta = 0.5$.

	$T = 1$		$T = 10$		$T = 20$		
N	$\|u - u_N^\beta\|_\infty$	$\|u - \tilde{u}_N^\beta\|_\infty$	$\|u - u_N^\beta\|_\infty$	$\|u - \tilde{u}_N^\beta\|_\infty$	$\|u - u_N^\beta\|_\infty$	$\|u - \tilde{u}_N^\beta\|_\infty$	CPU (s)
8	1.53e−03	6.34e−04	1.23e−02	1.01e−02	1.75e−01	3.83e−02	0.299341
16	7.15e−06	1.43e−05	7.05e−04	6.91e−04	8.01e−04	7.82e−04	0.334617
32	1.22e−09	1.31e−09	4.81e−08	4.71e−08	4.74e−08	4.74e−08	0.458201
64	1.58e−13	1.38e−13	6.82e−12	1.19e−13	2.09e−11	3.77e−13	0.942056

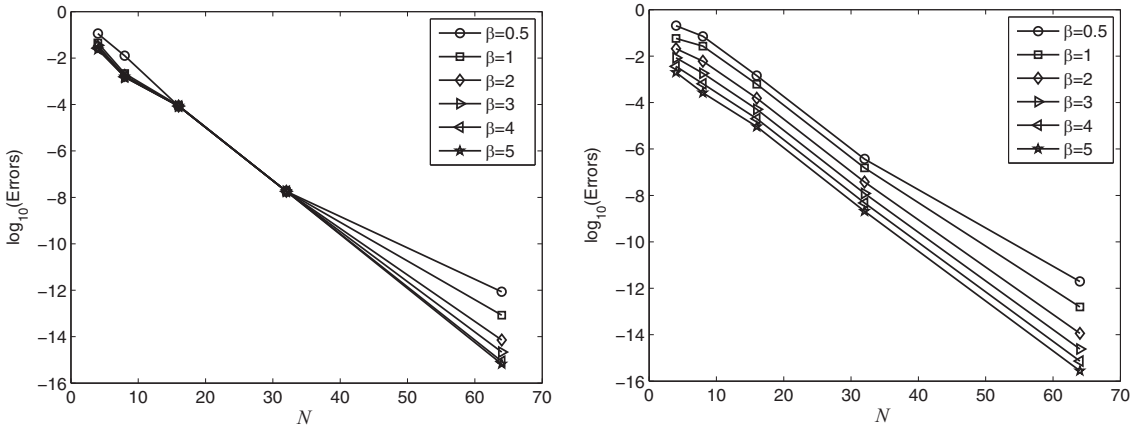

(A) log10 of maximum errors of the approximate solution

(B) $\log_{10}$ of $L^2_{w_\beta}$−errors of the approximate solution

FIGURE 4 Convergence rates of SLGR method with various β: Example 3 with $c_1 = 0.5$, $c_2 = 0.9$, and $T = 1$.

TABLE 8 The $L^2_{w_\beta}$-errors for Example 4 with $\beta = 0.9$.

N	8	16	32	64
$\|u - u_N^\beta\|_{w_\beta}$	1.09e−02	1.02e−03	5.18e−06	7.01e−11
$\|u - \tilde{u}_N^\beta\|_{w_\beta}$	1.09e−02	1.02e−03	5.18e−06	7.01e−11

Example 4. Consider the following WSVIEs with convolution kernel:

$$u(t) = f(t) + \lambda \int_0^t (t-s)^{-\frac{1}{2}} e^{-2(t-s)} u(s) ds,\ t \in [0, T], \tag{56}$$

where $f(t)$ is chosen so that the exact solution is $u(t) = te^{-2t}$, which is a fast decaying function. Tables 8 and 9 show the numerical errors versus N for $\lambda = 1/2$, obtained by using SLG scheme with $\beta = 0.9$. In Figure 8 (left), we plot $\log_{10}$ of the maximum error of the approximate solution, while on the right, we plot the corresponding $\log_{10}$ of the weighted error for $T = 8\pi$. It can be seen that if the solution decays exponentially, better numerical results can be obtained by choosing suitable $\beta > 1$, while conversely for the solution decaying very slowly (cf. Figure 3), where $u(t) = O(t^{-0.5})$.

Example 5. Consider

$$u(t) = \Gamma(2/3)t - \frac{1}{40}t^{\frac{8}{3}} + \frac{1}{27\Gamma(2/3)} \int_0^t s(t-s)^{-\frac{1}{3}} u(s) ds,\ t \in [0, 1], \tag{57}$$

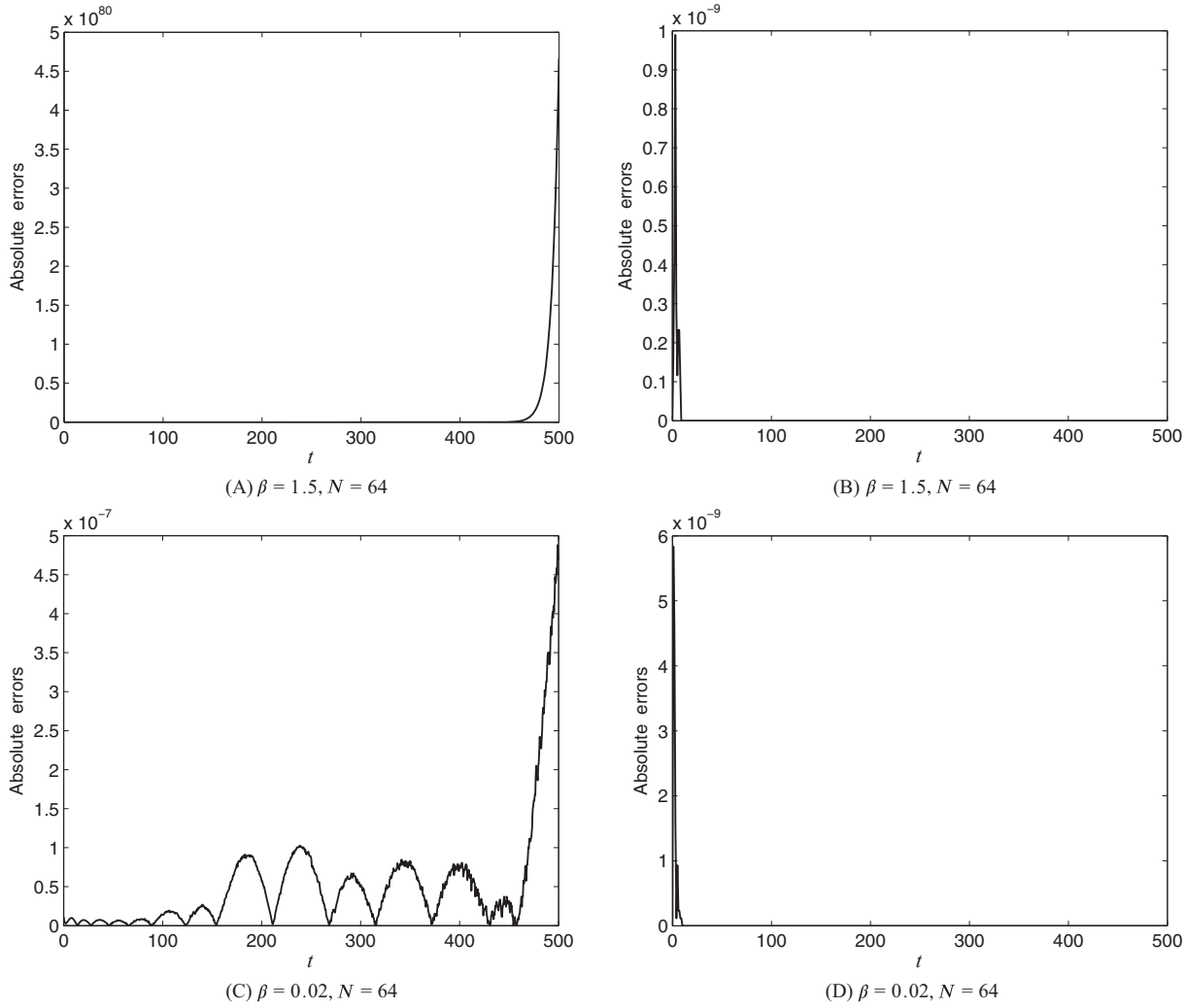

FIGURE 5 Plots of the absolute errors for approximate (left) and iterated (right) solutions of Example 3.

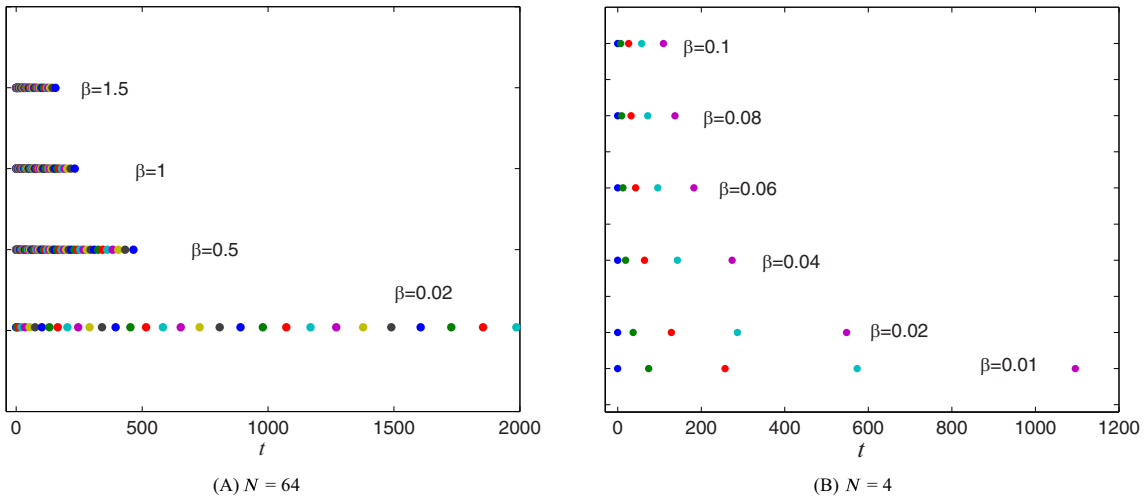

FIGURE 6 Effect of scaling factor β on the distribution of scaled Laguerre–Gauss–Radau nodes $\left\{\xi_{R,j}^{\beta,N}\right\}_{j=0}^{N}$ with respect to N. [Colour figure can be viewed at wileyonlinelibrary.com]

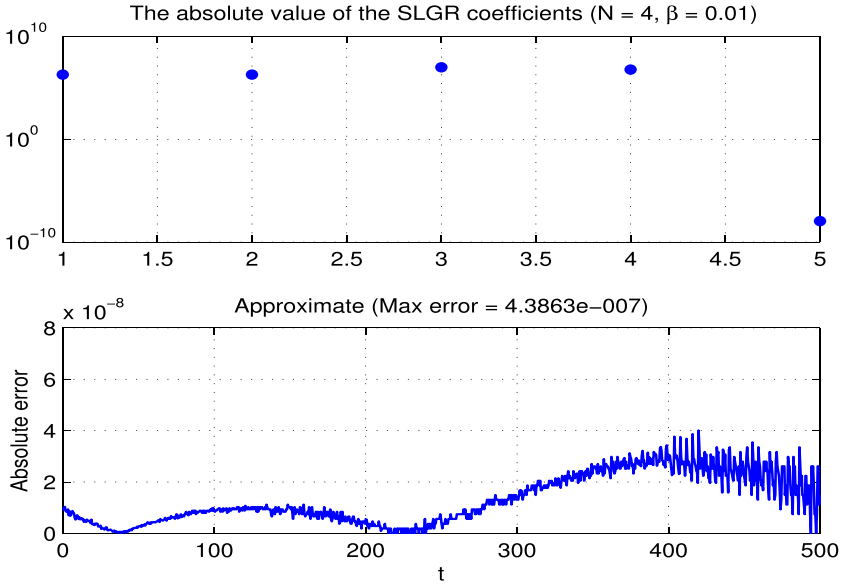

FIGURE 7 Additional numerical results of SLGR method: Example 3. [Colour figure can be viewed at wileyonlinelibrary.com]

TABLE 9 The maximum absolute errors and the CPU time for Example 4 with $\beta = 0.9$.

	$T = 1$		$T = 4\pi$		$T = 8\pi$		
N	$\|\|u - u_N^\beta\|\|_\infty$	$\|\|u - \tilde{u}_N^\beta\|\|_\infty$	$\|\|u - u_N^\beta\|\|_\infty$	$\|\|u - \tilde{u}_N^\beta\|\|_\infty$	$\|\|u - u_N^\beta\|\|_\infty$	$\|\|u - \tilde{u}_N^\beta\|\|_\infty$	CPU (s)
8	1.11e−01	1.93e−02	1.34e−01	7.79e−02	1.65e+01	9.74e+00	0.316834
16	1.14e−02	1.49e−03	2.51e−02	1.46e−02	1.90e+01	1.01e+00	0.345824
32	6.08e−05	5.70e−06	3.12e−04	1.40e−04	2.46e−02	1.17e−02	0.499355
64	8.49e−10	6.22e−11	6.22e−09	2.35e−09	7.98e−07	3.26e−07	0.999244

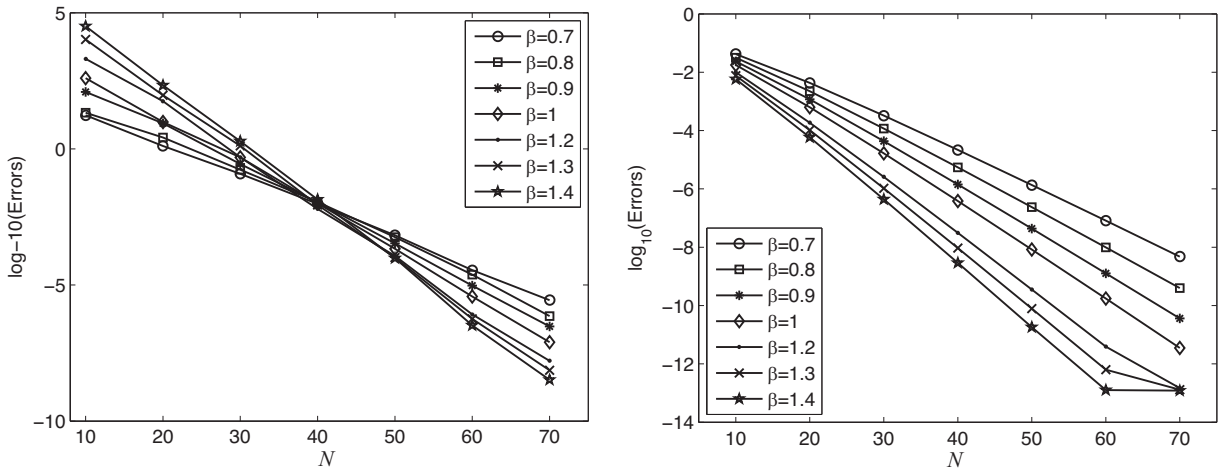

(A) $\log_{10}$ of maximum errors of the approximate solution with $T = 8\pi$

(B) $\log_{10}$ of $L^2_{w_\beta}-$errors of the approximate solution

FIGURE 8 Convergence rates of SLG method with various β: Example 4.

whose exact solution is $u(t) = \Gamma(2/3)t$. Table 10 shows that the numerical results obtained by using SLG scheme with $\beta = 2.5$ are much more better than those recently obtained by using the iterative method based on Picard iteration with a suitable quadrature formula in [35], as well as the Bernstein approximation method in [36].

	Proposed method				Method in [36]		Method in [35]
N	$\|u-u_N^\beta\|_\infty$	CPU (s)	$\|u-\tilde{u}_N^\beta\|_\infty$	CPU (s)	$\|e_N\|_\infty$	CPU (s)	$\|e_N\|_\infty$
12	1.96e−07	0.005201	1.96e−07	0.032897	1.71e−08	0.178833	2.49e−05
18	5.16e−10	0.009871	5.16e−10	0.059632	9.35e−08	0.237854	1.30e−05
24	1.19e−12	0.012802	1.19e−12	0.066287	1.23e−07	0.316412	6.04e−06

TABLE 10 Comparison of the maximum absolute errors for Example 5.

4 | CONCLUSION

In this paper, we developed and analyzed an efficient Galerkin spectral method using SLPs basis for WSVIEs on large intervals. The building block of the spectral algorithm is some appropriate variable transformations and the SLPs basis, where the inner products are evaluated by an appropriate quadrature rule. Using Young's inequality for convolution and some existing lemmas, we proved the spectral convergence of the approximate and iterated approximate solutions in the weighted L^2-norm. Numerical results show that the proposed method has better convergence rate and outperforms existing methods in terms of accuracy and efficiency. This is due to the great flexibility offered by the scaling parameter to fine-tune the spacing of collocation points. In addition, solving the WSVIEs on large intervals is important because it allows us to obtain more accurate and realistic solutions to a wide range of physical, biological, and engineering problems. This certainly provides a better understanding of the behavior of the underlying system. Clearly, it would be interesting and challenging to study nonlinear cases or other types of integral equations, such as those having variable coefficients in front of the integral operator.

AUTHOR CONTRIBUTIONS

Walid Remili: Conceptualization; investigation; data curation; formal analysis; visualization; validation. **Azedine Rahmoune:** Conceptualization; data curation; methodology; supervision; formal analysis; validation; investigation; visualization; writing—review and editing; writing—original draft; project administration. **Chenkuan Li:** Formal analysis; project administration; methodology; validation; investigation; visualization; funding acquisition.

ACKNOWLEDGEMENTS

The authors are thankful to the reviewers for giving valuable comments and suggestions.

CONFLICT OF INTEREST STATEMENT

The authors declare no potential conflict of interests.

ORCID

Azedine Rahmoune https://orcid.org/0000-0003-1267-6297
Chenkuan Li https://orcid.org/0000-0001-7098-8059

REFERENCES

1. A.-M. Wazwaz, *Linear and nonlinear integral equations: methods and applications*, Springer, Berlin, Heidelberg, 2011.
2. A.-M. Wazwaz and M. S. Mehanna, *The combined Laplace-Adomian method for handling singular integral equation of heat transfer*, Int. J. Nonlinear Sci. **10** (2010), no. 2, 248–252.
3. Y. I. Babenko, *Heat and mass transfer: a method for computing heat and diffusion flows*, Khimiya, Moscow, 1986.
4. R. Gorenflo and S. Vessella, *Abel integral equations: analysis and applications*, Springer, Berlin, Heidelberg, 1991.
5. E. G. Ladopoulos, *Singular integral equations: linear and non-linear theory and its applications in science and engineering*, Springer, Berlin, Heidelberg, 2013.
6. V. M. Aleksandrov and E. V. Kovalenko, *Mathematical method in the displacement problem*, Inzh. Zh. Mekh. Tverd. Tela. **2** (1984), 77–89.
7. H. Brunner, *On the numerical solution of first-kind Volterra integral equations with highly oscillatory kernels*, Isaac Newton Institute, HOP 13–17 September 2010, Highly Oscillatory Problems: From Theory to Applications.
8. H. J. T. Riele, *Collocation methods for weakly singular second-kind Volterra integral equations with non-smooth solution*, IMA J. Numer. Anal. **2** (1982), no. 4, 437–449.
9. H. Brunner and P. J. Houwen, *The numerical solution of Volterra equations*, North-Holland; Sole distributors for the U.S.A. and Canada, Elsevier Science Pub. Co., Amsterdam, New York, 1986.

10. H. Brunner, *Collocation methods for Volterra integral and related functional differential equations*, Cambridge Monographs on Applied and Computational Mathematics, Cambridge University Press, Cambridge, 2004.
11. H. Brunner, *Volterra integral equations: an introduction to theory and applications*, Cambridge Monographs on Applied and Computational Mathematics, Cambridge University Press, Cambridge, 2017.
12. A. Pedas and G. Vainikko, *Integral equations with diagonal and boundary singularities of the kernel*, Z. Anal. Anwend. **25** (2006), no. 4, 487–516.
13. F. de Hoog and R. Weiss, *On the solution of a Volterra integral equation with a weakly singular kernel*, SIAM J. Math. Anal. **4** (1973), no. 4, 561–573.
14. J. Abdalkhani, *A modified approach to the numerical solution of linear weakly singular Volterra integral equations of the second kind*, J. Integral Equ. Appl. **5** (1993), no. 2, 149–166.
15. C. Li and J. Beaudin, *Uniqueness of Abel's integral equations of the second kind with variable coefficients*, Symmetry **13** (2021), no. 6, 1064.
16. C. Li and H. M. Srivastava, *Uniqueness of solutions of the generalized Abel integral equations in Banach spaces*, Fractal Fract. **5** (2021), no. 3, 105.
17. H. Brakhage, K. Nickel, and P. Rieder, *Auflösung der abelschen integralgleichung 2. art*, Z. Angew. Math. Phys. (ZAMP) **16** (1965), 295–298.
18. A. M. Wazwaz and S. A. Khuri, *A reliable technique for solving the weakly singular second-kind Volterra-type integral equations*, Appl. Math. Comput. **80** (1996), no. 2, 287–299.
19. P. Polyanin and A. V. Manzhirov, *Handbook of integral equations*, 2nd ed., Chapman & Hall/CRC, New York, 2008.
20. Y. Chen and T. Tang, *Convergence analysis of the Jacobi spectral-collocation methods for Volterra integral equations with a weakly singular kernel*, Math. Comp. **79** (2010), 147–167.
21. M. Kolk, A. Pedas, and G. Vainikko, *High-order methods for Volterra integral equations with general weak singularities*, Numer. Funct. Anal. Optim. **30** (2009), no. 9–10, 1002–1024.
22. H. Liang and H. Brunner, *The convergence of collocation solutions in continuous piecewise polynomial spaces for weakly singular Volterra integral equations*, SIAM J. Numer. Anal. **57** (2019), no. 4, 1875–1896.
23. Z. Ma, A. A. Alikhanov, C. Huang, and G. Zhang, *A multi-domain spectral collocation method for Volterra integral equations with a weakly singular kernel*, Appl. Numer. Math. **167** (2021), 218–236.
24. M. N. Sahlan, H. R. Marasi, and F. Ghahramani, *Block-pulse functions approach to numerical solution of Abel's integral equation*, Cogent Math. **2** (2015), no. 1, 1047111.
25. L. Wang, H. Tian, and L. Yi, *An hp-version of the discontinuous Galerkin time-stepping method for Volterra integral equations with weakly singular kernels*, Appl. Numer. Math. **161** (2021), 218–232.
26. H. Liang, *Discontinuous Galerkin approximations to second-kind Volterra integral equations with weakly singular kernel*, Appl. Numer. Math. **179** (2022), 170–182.
27. S. Micula, *A numerical method for weakly singular nonlinear Volterra integral equations of the second kind*, Symmetry **12** (2020), no. 11, 1862.
28. E. Ashpazzadeh, Y.-M. Chu, M. S. Hashemi, M. Moharrami, and M. Inc, *Hermite multiwavelets representation for the sparse solution of nonlinear Abel's integral equation*, Appl. Math. Comput. **427** (2022), 127171.
29. M. R. Ali, M. M. Mousa, and W.-X. Ma, *Solution of nonlinear Volterra integral equations with weakly singular kernel by using the HOBW method*, Adv. Math. Phys. **2019** (2019), 1705651.
30. L. Zhu and Y. Wang, *Numerical solutions of Volterra integral equation with weakly singular kernel using SCW method*, Appl. Math. Comput. **260** (2015), 63–70.
31. H. Brezis, *Functional analysis, Sobolev spaces and partial differential equations*, Springer, New York, 2010.
32. G. Ben-Yu, W. Li-Lian, and W. Zhong-Qing, *Generalized Laguerre interpolation and pseudospectral method for unbounded domains*, SIAM J. Numer. Anal. **43** (2006), no. 6, 2567–2589.
33. G. Ben-yu and Z. Xiao-yong, *A new generalized Laguerre spectral approximation and its applications*, J. Comput. Appl. Math. **181** (2005), no. 2, 342–363.
34. K. E. Atkinson and W. Han, *Theoretical numerical analysis: a functional analysis framework*, Springer, New York, 2009.
35. S. Micula, *An iterative numerical method for fractional integral equations of the second kind*, J. Comput. Appl. Math. **339** (2018), 124–133.
36. F. Usta, *Numerical analysis of fractional Volterra integral equations via Bernstein approximation method*, J. Comput. Appl. Math. **384** (2021), 113198.

How to cite this article: W. Remili, A. Rahmoune, and C. Li, *Galerkin spectral method for linear second-kind Volterra integral equations with weakly singular kernels on large intervals*, Math. Meth. Appl. Sci. **47** (2024), 2329–2344, DOI 10.1002/mma.9750.